

Recent Stratospheric Climate Trends as Evidenced in Radiosonde Data: Global Structure and Tropospheric Linkages

DAVID W. J. THOMPSON

Department of Atmospheric Science, Colorado State University, Fort Collins, Colorado

SUSAN SOLOMON

National Oceanic and Atmospheric Administration/Aeronomy Laboratory, Boulder, Colorado

(Manuscript received 29 September 2004, in final form 23 June 2005)

ABSTRACT

The global structure of recent stratospheric climate trends is examined in radiosonde data. In contrast to conclusions published in previous assessments of stratospheric temperature trends, it is demonstrated that in the annual mean the tropical stratosphere has cooled substantially over the past few decades. The cooling of the tropical stratosphere is apparent in both nighttime and adjusted radiosonde data, and seems to be robust to changes in radiosonde instrumentation. The meridional structure of the annual-mean stratospheric trends is not consistent with our current understanding of radiative transfer and constituent trends but is consistent with increased upwelling in the tropical stratosphere.

The annual-mean cooling of the tropical stratosphere is juxtaposed against seasonally varying trends in the extratropical stratosphere dominated by the well-known springtime cooling at polar latitudes. The polar stratospheric trends are accompanied by similarly signed trends at tropospheric levels in the Southern Hemisphere but not in the Northern Hemisphere.

1. Introduction

The recent global-mean cooling of the stratosphere is widely viewed as evidence for a discernible anthropogenic impact on the climate system (e.g., WMO 1999, 2003; Ramaswamy et al. 2001; Ramaswamy and Schwarzkopf 2002; Shine et al. 2003; and references therein). From 1979 to 1994, global-mean stratospheric temperatures dropped by ~ 0.75 K decade⁻¹ in the stratosphere below ~ 35 km and ~ 2.5 K decade⁻¹ near 50 km, whereas the annually averaged global-mean rms variability in those regions is only ~ 0.2 and ~ 0.4 K, respectively (Ramaswamy et al. 2001). Attribution studies based on radiative/dynamical models suggest that stratospheric ozone depletion has accounted for much of the global-mean cooling in the extratropical lowermost stratosphere near 100 hPa, while both ozone depletion and increased carbon dioxide have contrib-

uted to the global temperature trends between 100 hPa and the stratopause (Langematz et al. 2003; Shine et al. 2003; and references therein). The role of stratospheric water vapor remains uncertain (Randel et al. 2004).

The amplitude of the observed stratospheric cooling is largest at polar latitudes during the spring season when temperatures have dropped by several degrees in both the Northern Hemisphere (NH) and Southern Hemisphere (SH) polar stratospheres since 1979 (Randel and Wu 1999; WMO 2003, chapter 3.1). The SH polar cooling is broadly consistent with ozone depletion driven by heterogeneous chemistry involving manmade chlorine occurring on polar stratospheric clouds (WMO 2003, chapter 3.4). The NH polar cooling is thought to reflect changes in atmospheric dynamics in addition to photochemical ozone losses and possible changes in water vapor (WMO 2003, chapter 3.4). Previous assessments of stratospheric temperature trends suggest that the tropical lower stratosphere is not cooling at a significant rate (e.g., Ramaswamy et al. 2001; WMO 2003).

Stratospheric temperature trends are of importance not only for their links to the stratospheric circulation but for their possible impacts on tropospheric climate

Corresponding author address: Dr. David W. J. Thompson, Department of Atmospheric Science, Colorado State University, Fort Collins, CO 80523.
E-mail: davet@atmos.colostate.edu

as well. Observations suggest that intraseasonal fluctuations in the extratropical stratospheric circulation are reflected at tropospheric levels in both the NH (Baldwin and Dunkerton 2001) and the SH (Graversen and Christiansen 2003; Thompson et al. 2005), and both observations and numerical results suggest that the stratospheric cooling associated with the Antarctic ozone hole has had a demonstrable impact on recent climate change at the earth's surface (Thompson and Solomon 2002; Gillett and Thompson 2003).

The purpose of the current study is to examine the global structure of recent stratospheric climate trends in current radiosonde data. The key result is that, in marked contrast with the conclusions reached in previous assessments of stratospheric temperature trends (e.g., Ramaswamy et al. 2001; WMO 2003), we find that in the annual mean the tropical stratosphere has cooled substantially over the past few decades. The results also imply that recent trends in the polar stratosphere are accompanied by analogous changes in the tropospheric circulation in the SH, but not in the NH.

2. Data

Trends were calculated for two radiosonde datasets: 1) monthly mean anomalies from the Integrated Global Radiosonde Archive (IGRA) and 2) monthly mean anomalies from the "liberal/conservative" ("LIBCON") adjusted radiosonde data published in Lanzante et al. (2003a,b, hereafter dataset referred to as LKS). The IGRA dataset is available from the Climate Analysis Branch at the National Oceanic and Atmospheric Administration (NOAA) National Climate Data Center and includes up-to-date monthly mean time series of temperature and geopotential height recorded at 0000 and 1200 UTC at hundreds of radiosonde stations distributed throughout the globe (Durre et al. 2005). The LKS dataset is available through 1997 and includes time series of temperature data at 87 radiosonde stations that have been adjusted to account for possible changes in radiosonde instrumentation (LKS). The detailed examination and adjustment of the radiosonde data described in Lanzante et al. (2003a) results in substantial changes in radiosonde records at certain stations, and hence the inclusion of the adjusted LKS data constitutes an important quality check on results derived from the unadjusted IGRA data.

Results were calculated for the unadjusted IGRA dataset and also for a merged dataset consisting of adjusted LKS data prior to 1997 supplemented by IGRA data between 1998 and 2003 (denoted combined LKS/

IGRA). Time series from the LKS and IGRA datasets were merged at all stations and levels as follows: First, the differences between the 1979–97 climatological means for the LKS and IGRA time series were subtracted from the IGRA time series as a function of calendar month. This procedure acts to center the anomalous IGRA time series about the same monthly varying climatology as the LKS time series during the period of overlap 1979–97. Second, any residual differences between the 1996–97 annual means for the LKS and centered IGRA time series were subtracted from the centered IGRA time series. This latter step ensures that adjustments made to the LKS time series prior to 1996 are also reflected in the combined LKS/IGRA time series. If there are no data available during 1996–97, the time series were not considered continuous and were not merged. The resulting combined LKS/IGRA dataset is analogous to the Radiosonde Atmospheric Temperature Products for Assessing Climate (RATPAC) dataset described in Free et al. (2005, manuscript submitted to *J. Geophys. Res.*).

Zonal means were obtained for the IGRA and combined LKS/IGRA datasets by averaging station data over latitude bands 10° in width, and area means were found by computing the cosine-weighted average of the zonal-mean time series over the appropriate latitude ranges. Results for the period of record following 1979 were calculated for radiosonde stations with at least 75% temporal coverage from 1979 to 2003, and results for the period of record starting at 1958 were calculated for stations with at least 66% coverage from 1958 to 2003.

The radiosonde archives are supplemented by data from the National Centers for Environmental Prediction–National Center for Atmospheric Research (NCEP–NCAR) reanalysis and satellite temperature retrievals from the Microwave Sounding Unit Channel 4 (MSU4) dataset. The NCEP–NCAR reanalysis data consist of numerous in situ and remotely sensed observations assimilated in an atmospheric general circulation model (Kalnay et al. 1996; Kistler et al. 2001). The MSU4 satellite temperature data used here are produced by the University of Alabama in Huntsville National Space and Technology Center and reflect a weighted average of atmospheric temperatures between the layer extending from ~ 300 to ~ 10 hPa, with maximum weighting centered at ~ 90 hPa (Spencer and Christy 1993). Note that the NCEP–NCAR reanalysis also includes assimilated MSU4 and radiosonde data and hence does not constitute an independent data source but is a useful check for physical consistency.

Linear trends were calculated for the period following 1979, which corresponds to the time interval when

the data coverage is most extensive in the radiosonde archives and also when satellite data are available and incorporated in the NCEP–NCAR reanalysis. Results were calculated at levels from 1000 to 10 hPa in the NCEP–NCAR reanalysis but because of the paucity of balloon measurements at 10 hPa, from 1000 to 30 hPa in the radiosonde data. In some illustrations presented below, results are highlighted at 70 hPa, which corresponds to the lowest standard level that lies in the stratosphere but above the height of the tropical tropopause. Note that the paucity of radiosonde data in the SH middle latitudes $\sim 35^{\circ}$ – 60° S implies that trends over this region should be treated with caution (Lanzante et al. 2003a,b).

The statistical significance of the trends and the associated confidence limits were assessed using a two-tailed test of the t statistic following Eqs. (1)–(5) of Santer et al. (2000). The methodology is analogous to assessing the significance of the correlation coefficient between the respective time series and the time axis. The effective number of degrees of freedom was estimated following the procedure outlined in section 5 of Bretherton et al. (1999). For year-round monthly mean radiosonde observations at 70 hPa, typical values of the effective number of degrees of freedom divided by the total sample size are ~ 0.85 in the extratropics and ~ 0.3 in the Tropics.

3. Results

a. Trends in annual-mean temperatures

Figure 1 shows trends in zonal-mean, annual-mean temperatures as a function of pressure level and latitude calculated for the period 1979–2003 from the combined LKS/IGRA data (top), the unadjusted IGRA data (middle), and the NCEP–NCAR reanalysis (bottom). The top two panels in Fig. 2 highlight the trends at 70 hPa for individual radiosonde stations. Three features in the combined LKS/IGRA trends are immediately apparent. First, the trends transition from warming to cooling near the height of the tropopause at all latitudes, with some evidence for cooling as low as 200 hPa in the equatorial region (Fig. 1, top). Second, the trends reveal enhanced annual-mean cooling in the SH polar stratosphere above ~ 200 hPa (Fig. 1, top). Third, the trends reveal substantial annual-mean cooling in the tropical stratosphere, with cooling minima located just outside the polar regions near 50° latitude (Fig. 1, top; Fig. 2a).

The principal features revealed in the stratospheric trends derived from the combined LKS/IGRA data

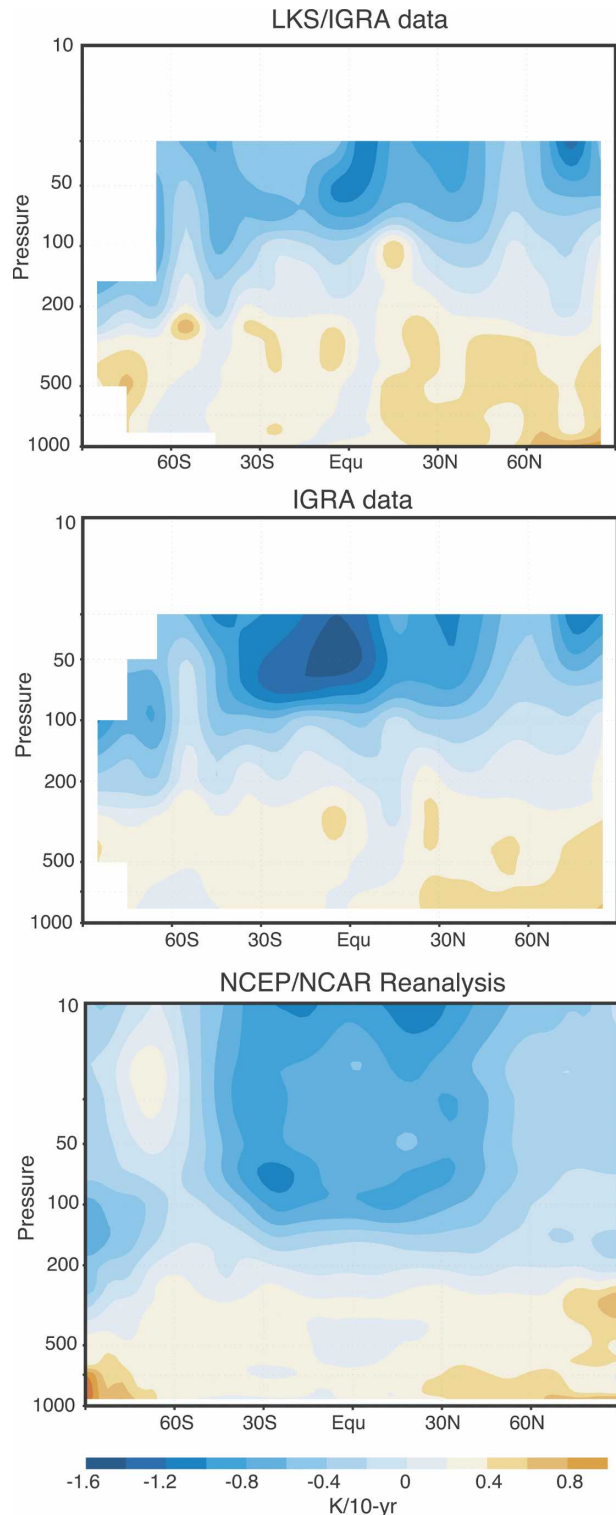
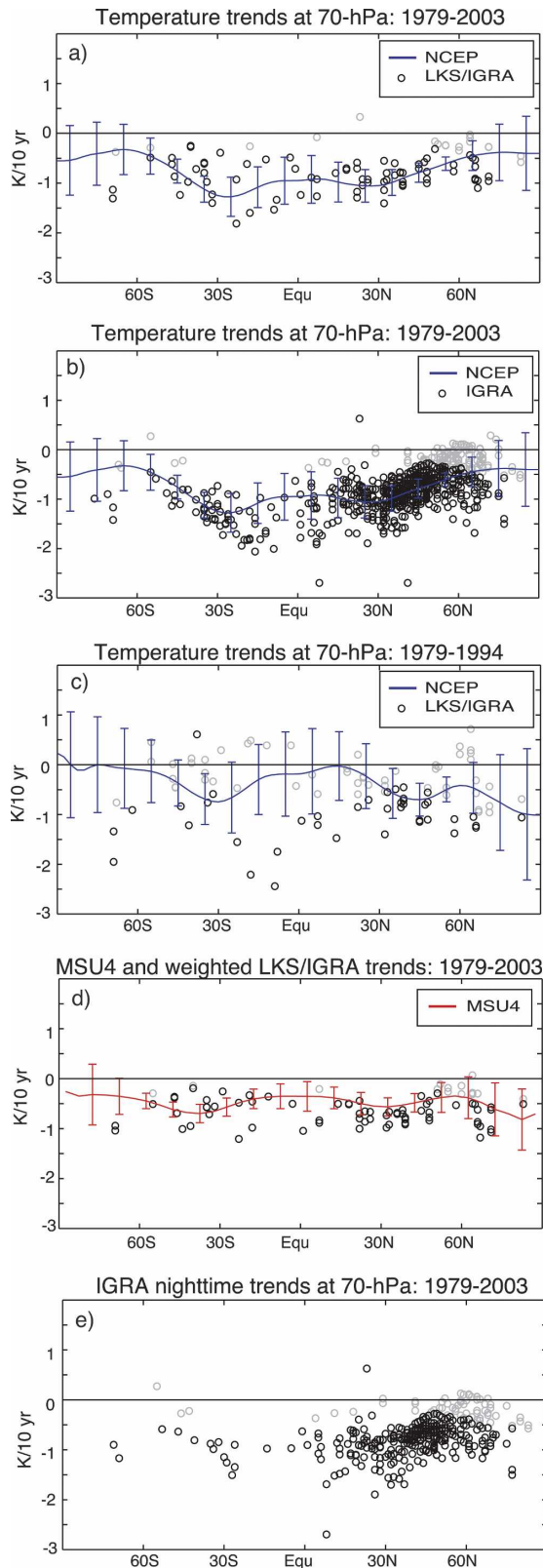


FIG. 1. Trends in zonal-mean, annual-mean temperature anomalies as a function of height and latitude for 1979–2003. Results are based on (top) radiosonde observations (raob) from the combined LKS/IGRA data, (middle) raob from the unadjusted IGRA dataset, and (bottom) the NCEP–NCAR reanalysis. Units: K decade^{-1} .



are also evident in the trends derived from the unadjusted IGRA data and the NCEP–NCAR reanalysis (Fig. 1, middle and bottom; Fig. 2b). The most obvious differences between trends in stratospheric temperatures in the three datasets are that 1) the unadjusted IGRA trends are somewhat larger than those found in the combined LKS/IGRA data in the tropical lower stratosphere, and 2) the tropical lower-stratospheric trends calculated for the reanalysis suggest a higher degree of hemispheric symmetry (with cooling maxima located in the subtropics near $\sim 30^{\circ}\text{N}$ and $\sim 30^{\circ}\text{S}$) than the radiosonde data.

The most striking feature in Fig. 1 and Figs. 2a,b is the widespread annual-mean cooling of the tropical lower stratosphere. The trends are substantial and statistically significant at nearly all radiosonde stations throughout a broad region extending from $\sim 40^{\circ}\text{S}$ to $\sim 40^{\circ}\text{N}$ (Figs. 2a,b). In contrast, the temperature trends are somewhat weaker and less significant at most stations in middle latitudes (Figs. 2a,b). The meridional structure of the stratospheric temperature trends does not exceed the error bars on the trends for individual latitude bands (e.g., Fig. 2a, blue lines), but the differences in cooling rates between tropical and middle latitudes are nevertheless readily evident in the pattern of the trends (Figs. 1 and 2a,b; Table 1) and also in time series of lower-stratospheric temperature anomalies averaged over the extended tropical ($40^{\circ}\text{--}40^{\circ}$) and extratropical ($40^{\circ}\text{--}90^{\circ}$) regions (Fig. 3, left and middle). The time series derived from the combined LKS/IGRA radiosonde data suggest that the tropical stratosphere has cooled for at least the past few decades, with the exception of two periods of transient warming associated with the eruptions of El Chichón and Pinatubo (Fig. 3, left). The tropical cooling is also evident in the individual radiosonde record afforded by Majuro, a record highlighted in Lanzante et al. (2003a), and nearby Truk

FIG. 2. (a) Same as in Fig. 1, but for trends at 70 hPa. Blue: trends based on the NCEP–NCAR reanalysis; circles: trends based on individual raobs from the combined LKS/IGRA data. Units: K decade^{-1} . Black circles denote trends that exceed the 95% confidence level. Error bars denote the 95% confidence level on the trends from the NCEP–NCAR reanalysis. (b) Same as in (a), but for raob from the unadjusted IGRA dataset. (c) Same as in (a), but for trends for 1979–94. (d) Same as in (a), but the red lines denote trends from the MSU4 dataset, and the black/gray circles denote radiosonde trends from the combined LKS/IGRA data that have been vertically averaged as per an MSU4 weighting function. Only radiosonde stations with coverage at all levels of 250–30 hPa are included in the MSU4 comparison. (e) Same as in (b), but for IGRA data restricted to nighttime hours.

TABLE 1. Trends in 70-hPa temperatures for datasets, periods, and latitude bands indicated. Bold font denotes trends that exceed the 95% confidence level. The trends in parentheses denote results for nighttime IGRA data only. Units: K decade⁻¹.

Temperature trends at 70 hPa from the combined LKS/IGRA data (K decade ⁻¹)				
	40°–90°S	40°N–40°S	40°–90°N	90°S–90°N
1979–2003	–0.76	–0.84	–0.57	–0.78
1979–94	–0.45	–0.51	–0.64	–0.53
Temperature trends at 70 hPa from the IGRA data (K decade ⁻¹)				
	40°–90°S	40°N–40°S	40°–90°N	90°S–90°N
1979–2003	–0.70 (–0.47)	–1.21 (–1.00)	–0.57 (–0.45)	–1.01 (–0.81)
1979–94	–0.45	–0.86	–0.65	–0.76
Temperature trends at 70 hPa from the NCEP–NCAR reanalysis (K decade ⁻¹)				
	40°–90°S	40°N–40°S	40°–90°N	90°S–90°N
1979–2003	–0.52	–1.04	–0.59	–0.87
1979–94	–0.17	–0.34	–0.61	–0.36

(Fig. 3, right). As evidenced in the top two panels of Fig. 4, the tropical-mean cooling exhibits a high degree of statistical significance and exceeds the global-mean cooling at levels above 100 hPa.

Previous studies have hinted at the substantial cooling of the tropical stratosphere revealed in Figs. 1–4. For example, Lanzante et al. (2003b) found a similar feature in trends based on adjusted radiosonde data at levels above ~100 hPa for the period 1959–97 (their Fig. 4, top left) and above ~50 hPa for the period 1979–

97 (their Fig. 4, top right). However, neither Lanzante et al. (2003b) nor other assessments have highlighted this feature for two likely reasons. First, several previous assessments of stratospheric temperature trends are based on periods of record ending in 1994 (e.g., Ramaswamy et al. 2001), whereas a comparison of the tropical-mean radiosonde temperature trends for different periods of record reveals that the inclusion of data since 1994 increases considerably both the amplitudes and significance levels of the trends in the low-

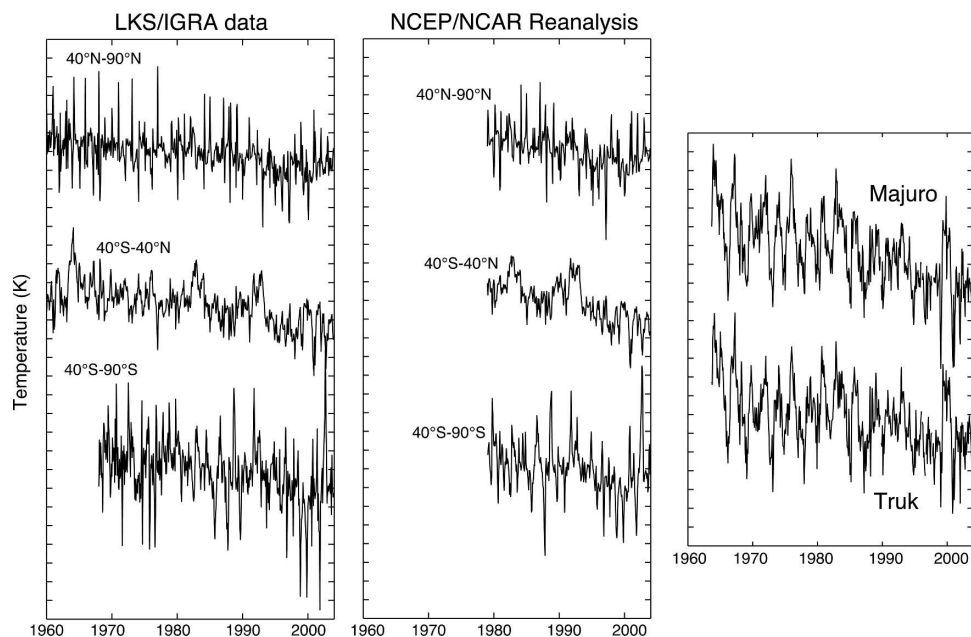
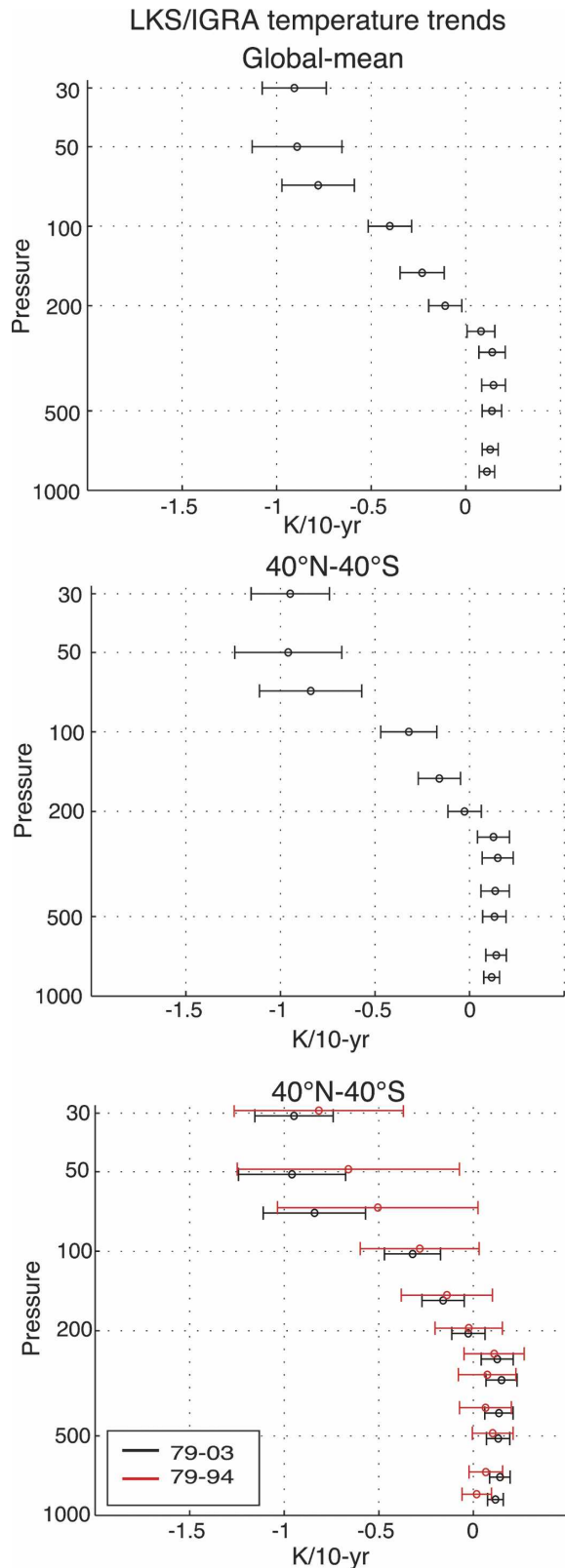


FIG. 3. Time series of zonal-mean temperature anomalies at 70 hPa for latitude bands indicated. (left) Time series based on radiosonde data from the combined LKS/IGRA data, (middle) time series based on the NCEP–NCAR reanalysis, and (right) time series for Majuro and Truk from the combined LKS/IGRA data. Tick marks: 1 K.



ermost tropical stratosphere (Fig. 2c; Fig. 4, bottom). The increased amplitudes and significance levels of the trends in the lowermost stratosphere are due in part to the absence of volcanic warming perturbations in the temperature record since the eruption of Mt. Pinatubo in 1991.

Second, previous assessments of stratospheric climate trends typically include analyses of remotely sensed temperature data such as those derived from the MSU4 instrument. The annually averaged trends in MSU4 data for 1979–2003 are shown as the red line in Fig. 2d. The MSU4 data reveal statistically significant cooling throughout much of the globe but do not suggest enhanced cooling in the tropical stratosphere (see also WMO 2003, chapter 4.4). However, as presented in Fig. 2d, when an MSU4 weighting function (obtained from Remote Sensing Systems online at <http://www.remss.com>) is applied to the individual radiosonde stations, the meridional structure of the resulting weighted radiosonde trends is substantially diminished, particularly at tropical latitudes. The absence of a tropical cooling maximum in the MSU4 data is thus consistent with the facts that 1) the MSU4 data reflect an average over a layer where the temperature trends in the IGRA data exhibit a sharp vertical gradient, and 2) the weighting function for the MSU4 data includes a larger fraction of the upper troposphere at tropical latitudes than it does at extratropical latitudes (see also Angell 2003).

Previous studies have also stressed uncertainties inherent in radiosonde data (e.g., Parker et al. 1997; Gaffen et al. 2000; Lanzante et al. 2003a,b; Seidel et al. 2004), and both discontinuities and systematic errors are known to impact trend estimates (e.g., Ramaswamy et al. 2001, and references therein). For example, changes in radiosonde instrumentation have affected the radiation correction for stratospheric temperatures (Elliott et al. 2002), and these changes can result in spurious daytime cooling at stratospheric levels (Seidel et al. 2001). Additionally, the NCEP–NCAR reanalysis exhibits an apparent discontinuity in temperatures near the tropical tropopause around 2001, and this is thought to reflect changes in the satellite radiance data input to the reanalysis (Randel et al. 2004). Nevertheless, the

←

FIG. 4. Vertical profiles of temperature trends averaged over (top) the globe and (middle) the extended tropical region (40°N–40°S) for 1979–2003. (bottom) Same as in the middle panel, but results highlighted in red correspond to the period 1979–94. Trends based on radiosonde data from the combined LKS/IGRA data. The error bars denote the 95% confidence level. Units: K decade^{−1}.

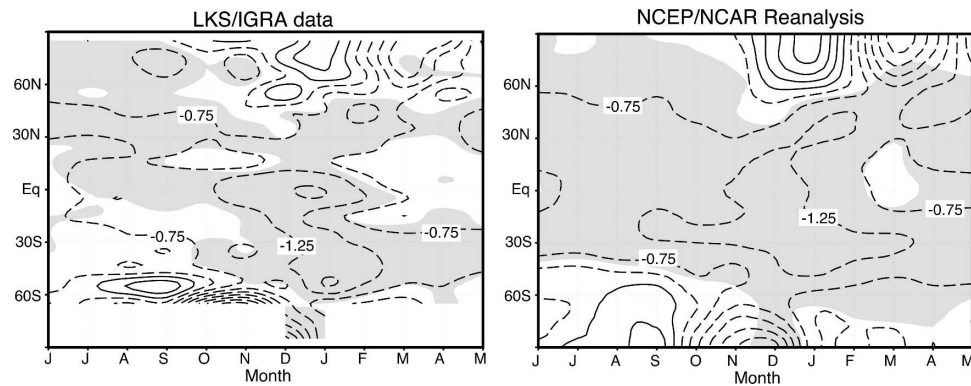


FIG. 5. Trends in 70-hPa zonal mean temperature anomalies for 1979–2003. Trends are shown as a function of month and latitude. (left) Trends based on radiosonde data from the combined LKS/IGRA data; (right) trends based on the NCEP–NCAR reanalysis. Shading denotes trends that exceed the 95% confidence level. Tick marks on the ordinate axis denote the center of the respective month. Units: K decade^{-1} ($-0.25, 0.25, 0.75 \dots$).

tropical cooling highlighted in Figs. 1–4 is strongly supported by the following observations:

- 1) the tropical cooling is clearly evident and statistically significant at virtually all tropical radiosonde stations in both adjusted and unadjusted data (Figs. 2a,b);
- 2) the meridional structure of the stratospheric temperature trends is evident in IGRA data restricted to nighttime hours (Table 1; Fig. 2e) and is thus robust to changes in the daytime radiation correction applied to radiosonde data;
- 3) time series of both individual and tropical-mean stratospheric temperatures reveal that the tropical cooling does not reflect any obviously anomalous step functions in the data (Fig. 3);
- 4) the tropical cooling revealed in the NCEP–NCAR reanalysis is evident in trends calculated for 1979–2000 (not shown) and is thus not dominated by step changes in that data during 2001; and
- 5) the tropical cooling rate is robust to changes in the start and end points of the analysis, albeit with differences in statistical significance for analyses ending shortly after the eruption of Mt. Pinatubo, as noted above. Tropical cooling trends are also obtained for periods of record ending in 1997 (i.e., as used in Lanzante et al. 2003b) and for periods of record starting in 1985 (i.e., following the warming associated with El Chichón; not shown).

b. Seasonally varying structure of the trends

The seasonally varying structure of the lower-stratospheric temperature trends (Figs. 5 and 6) reveals that the cooling of the tropical stratosphere is evident during all calendar months, with a weak cooling maxi-

mum found between ~November and ~January. Recent polar stratospheric trends exhibit a more marked seasonality, with enhanced cooling during the spring months preceded by weak warming during early to mid-winter (Fig. 5; Fig. 6, top). The tropical trends are slightly larger than the extratropical trends during all calendar months except for the late-spring season (Fig. 6). The warming of the polar stratosphere during early to midwinter is not statistically significant in either hemisphere (Fig. 5), but the juxtaposition of this feature alongside springtime cooling in both hemispheres gives rise to an apparent hemispheric symmetry in the seasonality of recent polar stratospheric trends (Fig. 6, top).

The springtime cooling of the polar stratosphere has been primarily linked to photochemical ozone depletion in the SH (Randel and Wu 1999; Langematz et al. 2003; WMO 2003, chapter 3.4) and to decreased stratospheric wave driving in conjunction with photochemical ozone depletion in the NH (Langematz et al. 2003; WMO 2003, chapter 3.4). The warming of the NH polar stratosphere during early winter is consistent with the recent increase of early winter wave driving there (Randel et al. 2002; Manney et al. 2005), whereas the weak warming of the SH polar stratosphere during September reflects the SH sudden warming of September 2002 (see the special issue of the *Journal of the Atmospheric Sciences*, 2005, Vol. 62, No. 3). The lack of significance in the cooling trends in SH polar regions during October and November reflects the impact of the SH sudden warming of 2002 on the amplitude and significance of recent trends estimates.

The vertical structure of the seasonally varying polar trends is examined in Fig. 7. The top panels show trends in the IGRA temperature data averaged 60° – 90° N

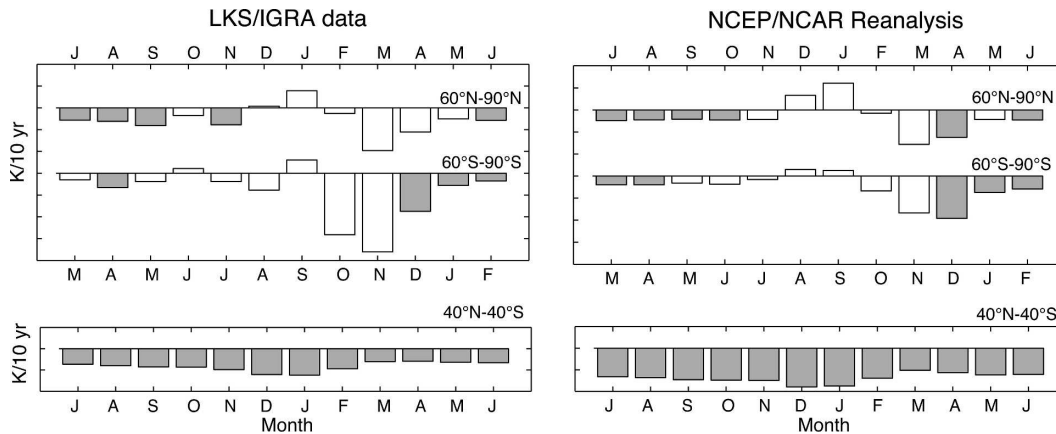


FIG. 6. (top) Linear trends in temperature anomalies at 70 hPa averaged over 60°–90°N (top bars) and 60°–90°S (bottom bars) for 1979–2003 (K decade^{-1}). Trends are shown as a function of month. (bottom) Same as in the top, but for temperatures averaged over 40°N–40°S. (left) Trends based on radiosonde data from the combined LKS/IGRA data and (right) trends based on the NCEP–NCAR reanalysis. Trends that exceed the 95% confidence level are shaded. Tick marks on the ordinate axis denote the center of the respective month. Note that the NH ordinate axis is shifted relative to the SH ordinate axis. Tickmarks: 1 K decade^{-1} .

(left) and 60°–90°S (right); the bottom panels show trends in the IGRA geopotential height data averaged over these same regions. Since the variance in geopotential height is largest over the polar cap, the time series of geopotential height anomalies averaged poleward of 60°N and 60°S correspond closely to the strength of the zonal flow averaged along $\sim 60^\circ$ and also to variations in the Northern and Southern Hemisphere annular modes, respectively. The results in Fig. 7 are based on the IGRA data since geopotential height data is not available for the LKS archive, but similar polar temperature trends are obtained for temperature data from the combined LKS/IGRA data (not shown).

As noted above, recent SH polar stratospheric trends are dominated by springtime cooling and hence a strengthening of the SH polar vortex (right panels), whereas recent NH polar stratospheric trends are characterized by rising geopotential heights and temperatures during \sim December–January but falling geopotential heights and temperatures during \sim March (left panels). Consistent with results reported in Thompson and Solomon (2002), the springtime strengthening and cooling of the SH polar stratospheric vortex precedes similarly signed changes in the SH tropospheric circulation by \sim one month (bottom right panel). The barotropic nature of the SH trends suggests they reflect dynamical coupling between the stratospheric and tropospheric circulations. An analogous relationship is not apparent in the NH, where both the early winter geopotential height rises and springtime geopotential height falls appear to follow rather than precede similarly signed changes in the polar troposphere (bottom left).

The results in Fig. 7 thus highlight two key aspects of recent NH climate trends. First, the widely cited falls in NH polar pressures during January–March (i.e., the trend toward the high index polarity of the Northern Annular Mode/North Atlantic Oscillation) are preceded by comparable rises in polar geopotential heights during \sim November–December (Fig. 7, bottom left). Second, recent trends in the NH troposphere are not associated with similarly signed changes in the NH polar stratosphere in a manner consistent with that observed in the SH.

4. Discussion

The results in this study support previous findings that the global lower stratosphere has cooled substantially since 1979 and that both the NH and SH polar stratospheres have cooled more than the global average during the spring season (WMO 2003, chapters 3.1 and 4.4). However, the results also reveal the following novel findings: 1) in the annual mean, the tropical stratosphere is cooling at a substantial rate and; 2) the seasonally varying trends in the polar stratosphere are associated with similarly signed trends in the troposphere in the SH but not in the NH. The observed structure in the annual-mean stratospheric temperature trends is particularly surprising since it contradicts the conclusion reached in WMO (2003) that only the extratropical stratosphere is cooling at a significant rate.

Is the cooling of the tropical stratosphere an artifact of the radiosonde data and the NCEP–NCAR reanalysis? As discussed in section 3, both the radiosonde data

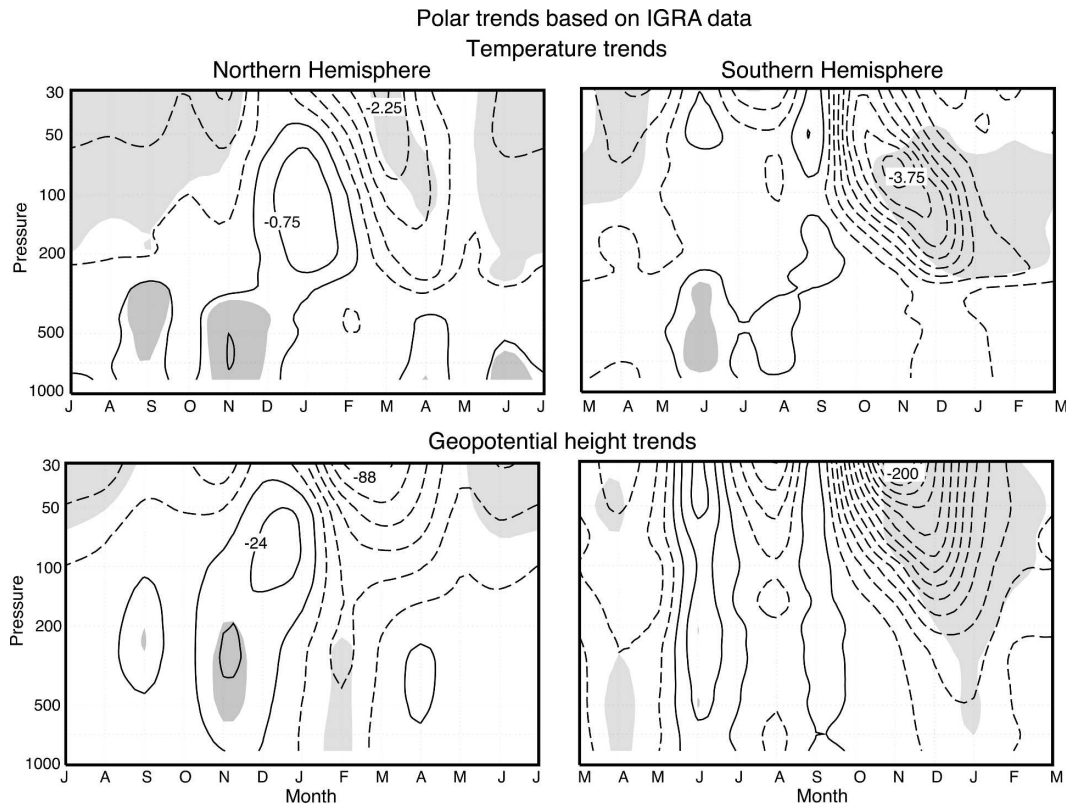


FIG. 7. Trends in (top) temperature and (bottom) geopotential height anomalies averaged over (left) 60° – 90° N and (right) 60° – 90° S for 1979–2003. Trends are shown as a function of month and pressure level. Shading denotes trends that exceeded the 95% confidence level. Tick marks on the ordinate axis denote the center of the respective month. Note that the NH ordinate axis is shifted relative to the SH ordinate axis. Trends based on radiosonde data from the IGRA. Units: K decade^{-1} ($-0.25, 0.25, 0.75 \dots$) and m decade^{-1} ($-8, 8, 24 \dots$).

and the NCEP–NCAR reanalysis are known to exhibit discontinuities at various times in the observational record. Nevertheless, the tropical stratospheric cooling is strongly supported by a number of observations, including the facts that 1) the cooling is evident and statistically significant at virtually all radiosonde stations, including both adjusted data (Fig. 2a) and unadjusted data restricted to nighttime hours (Fig. 2e); 2) the cooling is visually apparent in time series for individual radiosonde stations (Fig. 3); and 3) time series of stratospheric temperatures averaged over the extended tropical region do not reflect any obviously anomalous step functions in the data (Fig. 3). As noted in section 3, a tropical cooling maximum is not evident in the MSU4 data, but the differences between the MSU4 and radiosonde temperature trends are consistent with the fact the MSU4 data reflect a substantial fraction of the troposphere at tropical latitudes.

What processes may underlie a tropical maximum in annual-mean stratospheric cooling? Changes in the composition of the stratosphere undoubtedly play an

important role in global-mean stratospheric temperature trends and in the enhanced springtime cooling of the polar stratosphere (Shine et al. 2003; WMO 2003, chapter 3.4). However, tropical stratospheric cooling is not evident in the simulated response to observed trends in ozone and well-mixed greenhouse gases at levels below 10 hPa (Ramaswamy and Schwarzkopf 2002; Shine et al. 2003). Published observational and modeling studies suggest that there are insufficient levels of reactive halogen gases in the Tropics to initiate widespread chemical ozone depletion in that region (WMO 2003, chapters 1 and 4). Additionally, increased concentrations of carbon dioxide favor relatively weak cooling in the tropical lower stratosphere, since increased emissivity acts on relatively low climatological mean temperatures there. Increases in stratospheric water vapor may also contribute to a meridional gradient in stratospheric cooling (Forster and Shine 1999), but trends in this trace gas remain uncertain (Randel et al. 2004).

An alternative mechanism for the observed tropical

stratospheric temperature trends is adiabatic cooling driven by enhanced upwelling in the tropical stratosphere. Upwelling in the lower and middle tropical stratosphere is primarily driven by waves that propagate upward from the troposphere and break at stratospheric levels (e.g., Holton et al. 1995; Semeniuk and Shepherd 2001). An increase in stratospheric wave driving is implied in several simulations of the climate response to increasing greenhouse gases (e.g., Butchart and Scaife 2001; Gillett et al. 2003; Langematz et al. 2003), but such a response is typically weak and is not robust in all climate models (e.g., Austin et al. 2003).

It is noteworthy that an increase in upwelling would also act to decrease lower tropical stratospheric ozone levels via the enhanced transport of ozone-poor air from the tropical tropopause region. This effect would act to further exacerbate the cooling of the tropical stratosphere through the decreased absorption of radiation. Unfortunately, in the Tropics, satellite retrievals of total column ozone primarily reflect ozone levels in the middle and upper stratosphere, and profile data are scarce (Randel et al. 1999).

The structure of the annual-mean stratospheric temperature trends revealed in this study has implications for not only the amplitude and attribution of current global-mean temperature trends but also for large-scale trends in the atmospheric circulation. The results underscore the importance of considering both stratospheric and tropospheric processes, and the coupling between them, in the interpretation of recent climate change.

Acknowledgments. Thanks to W. Randel and two anonymous referees for insightful comments on the manuscript. Thanks also to D. Siedel for helpful comments on the manuscript and suggesting the use of the LKS data; to I. Durre for providing the IGRA dataset; to J. Lanzante, S. Klein, and D. Seidel for providing the LKS data; to F. Wu for assistance with the MSU4 data; and to P. Forster, G. Reid, W. Robinson, and K. Rosenlof for useful suggestions on the manuscript. The NCEP–NCAR reanalysis was obtained from the NOAA Climate Diagnostics Center. DWJT is supported by the NSF Climate Dynamics program through Grants NSF CAREER: ATM-0132190 and NSF ATM-0320959.

REFERENCES

- Angell, J. K., 2003: Effect of exclusion of anomalous tropical stations on temperature trends from a 63-station radiosonde network, and comparison with other analyses. *J. Climate*, **16**, 2288–2295.
- Austin, J., and Coauthors, 2003: Uncertainties and assessments of chemistry–climate models of the stratosphere. *Atmos. Chem. Phys.*, **3**, 1–27.
- Baldwin, M. P., and T. J. Dunkerton, 2001: Stratospheric harbingers of anomalous weather regimes. *Science*, **294**, 581–584.
- Bretherton, C. S., M. Widmann, V. P. Dymnikov, J. M. Wallace, and I. Bladé, 1999: The effective number of spatial degrees of freedom of a time-varying field. *J. Climate*, **12**, 1990–2009.
- Butchart, N., and A. A. Scaife, 2001: Removal of chlorofluorocarbons by increased mass exchange between the stratosphere and troposphere in a changing climate. *Nature*, **410**, 799–802.
- Durre, I., R. S. Vose, and D. B. Wuertz, 2005: Overview of the integrated global radiosonde archive. *J. Climate*, in press.
- Elliott, W. P., R. J. Ross, and W. H. Blackmore, 2002: Recent changes in NWS upper-air observations with emphasis on changes from VIZ to Vaisala radiosondes. *Bull. Amer. Meteor. Soc.*, **83**, 1003–1017.
- Forster, P. M. de F., and K. P. Shine, 1999: Stratospheric water vapor changes as a possible contributor to observed stratospheric cooling. *Geophys. Res. Lett.*, **26**, 3309–3312.
- Gaffen, D. J., M. A. Sargent, R. E. Habermann, and J. R. Lanzante, 2000: Sensitivity of tropospheric and stratospheric temperature trends to radiosonde data quality. *J. Climate*, **13**, 1776–1796.
- Gillett, N. P., and D. W. J. Thompson, 2003: Simulation of recent Southern Hemisphere climate change. *Science*, **302**, 273–275.
- , M. R. Allen, and K. D. Williams, 2003: Modelling the atmospheric response to doubled CO₂ and depleted stratospheric ozone using a stratosphere-resolving coupled GCM. *Quart. J. Roy. Meteor. Soc.*, **129**, 947–966.
- Graversen, R., and B. Christiansen, 2003: Downward propagation from the stratosphere to the troposphere: A comparison of the two hemispheres. *J. Geophys. Res.*, **108**, 4780, doi:10.1029/2003JD004077.
- Holton, J. R., P. H. Haynes, M. E. McIntyre, A. R. Douglass, R. B. Rood, and L. Pfister, 1995: Stratosphere-troposphere exchange. *Rev. Geophys.*, **33**, 403–440.
- Kalnay, M. E., and Coauthors, 1996: The NCEP/NCAR 40-Yr Reanalysis Project. *Bull. Amer. Meteor. Soc.*, **77**, 437–471.
- Kistler, R., and Coauthors, 2001: The NCEP–NCAR 50-year reanalysis: Monthly means CD-ROM and documentation. *Bull. Amer. Meteor. Soc.*, **82**, 247–268.
- Langematz, U., M. Kunze, K. Krüger, K. Labitzke, and G. L. Roff, 2003: Thermal and dynamical changes of the stratosphere since 1979 and their link to ozone and CO₂ changes. *J. Geophys. Res.*, **108**, 4027, doi:10.1029/2002JD002069.
- Lanzante, J. R., S. A. Klein, and D. J. Seidel, 2003a: Temporal homogenization of monthly radiosonde temperature data. Part I: Methodology. *J. Climate*, **16**, 224–240.
- , —, and —, 2003b: Temporal homogenization of monthly radiosonde temperature data. Part II: Trends, sensitivities, and MSU comparison. *J. Climate*, **16**, 241–262.
- Manney, G. L., K. Kruger, J. Sabutis, S. A. Sena, and S. Pawson, 2005: The remarkable 2003–2004 winter and other recent warm winters in the Arctic stratosphere since the late 1990s. *J. Geophys. Res.*, **110**, D04107, doi:10.1029/2004JD005367.
- Parker, D. E., M. Gordon, D. P. N. Cullum, D. M. H. Sexton, C. K. Folland, and N. Rayner, 1997: A new global gridded radiosonde temperature data base and recent temperature trends. *Geophys. Res. Lett.*, **24**, 1499–1502.
- Ramaswamy, V., and M. D. Schwarzkopf, 2002: Effects of ozone and well-mixed gases on annual-mean stratospheric temperature trends. *Geophys. Res. Lett.*, **29**, 2064, doi:10.1029/2002GL015141.

- , and Coauthors, 2001: Stratospheric temperature trends: Observations and model simulations. *Rev. Geophys.*, **39**, 71–122.
- Randel, W. J., and F. Wu, 1999: Cooling of the Arctic and Antarctic polar stratospheres due to ozone depletion. *J. Climate*, **12**, 1467–1479.
- , R. S. Stolarski, D. H. Cunnold, J. A. Logan, M. J. Newchurch, and J. M. Zawodny, 1999: Trends in the vertical distribution of ozone. *Science*, **285**, 1689–1692.
- , F. Wu, and R. Stolarski, 2002: Changes in column ozone correlated with the stratospheric EP flux. *J. Meteor. Soc. Japan*, **80**, 849–862.
- , —, S. J. Oltmans, K. Rosenlof, and G. E. Nedoluha, 2004: Interannual changes of stratospheric water vapor and correlations with tropical tropopause temperatures. *J. Atmos. Sci.*, **61**, 2133–2148.
- Santer, B. D., T. M. L. Wigley, J. S. Boyle, D. J. Gaffen, J. J. Hnilo, D. Nychka, D. E. Parker, and K. E. Taylor, 2000: Statistical significance of trend differences in layer-average temperature time series. *J. Geophys. Res.*, **105**, 7337–7356.
- Seidel, D. J., R. J. Ross, J. K. Angell, and G. C. Reid, 2001: Climatological characteristics of the tropical tropopause as revealed by radiosondes. *J. Geophys. Res.*, **106**, 7857–7878.
- , and Coauthors, 2004: Uncertainty in signals of large-scale climate variations in radiosonde and satellite upper-air temperature datasets. *J. Climate*, **17**, 2225–2240.
- Semeniuk, K., and T. G. Shepherd, 2001: Mechanisms for tropical upwelling in the stratosphere. *J. Atmos. Sci.*, **58**, 3097–3115.
- Shine, K. P., and Coauthors, 2003: A comparison of model-simulated trends in stratospheric temperatures. *Quart. J. Roy. Meteor. Soc.*, **129**, 1565–1588.
- Spencer, R. W., and J. R. Christy, 1993: Precision lower stratospheric temperature monitoring with the MSU: Technique, validation and results, 1979–1991. *J. Climate*, **6**, 1194–1204.
- Thompson, D. W. J., and S. Solomon, 2002: Interpretation of recent Southern Hemisphere climate change. *Science*, **296**, 895–899.
- , M. P. Baldwin, and S. Solomon, 2005: Stratosphere–troposphere coupling in the Southern Hemisphere. *J. Atmos. Sci.*, **62**, 708–715.
- World Meteorological Organization, 1999: Scientific assessment of ozone depletion: 1998. Global Ozone Research and Monitoring Project Rep. 44, Geneva, Switzerland, 546 pp.
- , 2003: Scientific assessment of ozone depletion: 2002. Global Ozone Research and Monitoring Project Rep. 47, Geneva, Switzerland, 498 pp.